



RESEARCH ARTICLE

10.1002/2015EA000107

Key Points:

- GEBCO_2014, a digital global bathymetric model, is documented
- Thirty-three percent of ocean grid cells have been updated from previous version
- Updated regional bathymetric compilations and other data incorporated

Correspondence to:

K. M. Marks,
Karen.Marks@noaa.gov

Citation:

Weatherall P., K. M. Marks, M. Jakobsson, T. Schmitt, S. Tani, J. E. Arndt, M. Rovere, D. Chayes, V. Ferrini, and R. Wigley (2015), A new digital bathymetric model of the world's oceans, *Earth and Space Science*, 2, doi: 10.1002/2015EA000107.

Received 2 APR 2015

Accepted 24 JUN 2015

Accepted article online 29 JUN 2015

A new digital bathymetric model of the world's oceans

Pauline Weatherall¹, K. M. Marks², Martin Jakobsson³, Thierry Schmitt⁴, Shin Tani⁵, Jan Erik Arndt⁶, Marzia Rovere⁷, Dale Chayes⁸, Vicki Ferrini⁸, and Rochelle Wigley⁹

¹British Oceanographic Data Centre, Liverpool, UK, ²NOAA Laboratory for Satellite Altimetry, College Park, Maryland, USA, ³Department of Geological Sciences, Stockholm University, Stockholm, Sweden, ⁴Service Hydrographique et Océanographique de la Marine, Brest, France, ⁵Hydrographic and Oceanographic Department, Japan Coast Guard (Retired), Tokyo, Japan, ⁶Alfred Wegener Institute für Polar-und Meeresforschung, Bremerhaven, Germany, ⁷Institute for Marine Sciences, Consiglio delle Ricerche, Bologna, Italy, ⁸Lamont-Doherty Earth Observatory of Columbia University, Palisades, New York, USA, ⁹Center for Coastal and Ocean Mapping, University of New Hampshire, Durham, New Hampshire, USA

Abstract General Bathymetric Chart of the Oceans (GEBCO) has released the GEBCO_2014 grid, a new digital bathymetric model of the world ocean floor merged with land topography from publicly available digital elevation models. GEBCO_2014 has a grid spacing of 30 arc sec and updates the 2010 release (GEBCO_08) by incorporating new versions of regional bathymetric compilations from the International Bathymetric Chart of the Arctic Ocean, the International Bathymetric Chart of the Southern Ocean, the Baltic Sea Bathymetry Database, and data from the European Marine Observation and Data network bathymetry portal, among other data sources. Approximately 33% of ocean grid cells (not area) have been updated in GEBCO_2014 from the previous version, including both new interpolated depth values and added soundings. These updates include large amounts of multibeam data collected using modern equipment and navigation techniques, improving portrayed details of the world ocean floor. Of all nonland grid cells in GEBCO_2014, approximately 18% are based on bathymetric control data, i.e., primarily multibeam and single-beam soundings or preprepared grids which may contain some interpolated values. The GEBCO_2014 grid has a mean and median depth of 3897 m and 3441 m, respectively. Hypsometric analysis reveals that 50% of the Earth's surface is composed of seafloor located 3200 m below mean sea level and that ~900 ship years of surveying would be needed to obtain complete multibeam coverage of the world's oceans.

1. Introduction

Bathymetry refers to the underwater depth of lake or ocean floor. It comprises the geospatial framework equivalent to land topography and therefore constitutes a critical boundary condition for geophysical, geological, biological, and oceanographic systems. However, because of the difficulty of mapping through water, what we know about the shape of the ocean floor is lagging behind our knowledge of land topography.

The importance of knowing the physical dimensions, characteristics, and shape of the ocean floor was acknowledged more than a century ago by HSH Prince Albert I of Monaco who, in 1903, initiated the General Bathymetric Chart of the Oceans (GEBCO) with the goal of mapping the bathymetry of the world's oceans [Hall, 2006]. The oceans were divided into "plotting sheets" which were assigned to cartographers or, more aptly titled, to "bathymetrists." From plotted ship soundings they portrayed the shape of the ocean floor by drawing depth contours, or "isobaths," onto a bathymetric map sheet. In 1973, GEBCO was transformed into a program under the auspices of the International Hydrographic Organization (IHO) and Intergovernmental Oceanographic Commission (IOC) of the United Nations Educational, Scientific, and Cultural Organization. The last set of printed map sheets, the GEBCO Fifth Edition, were published during the 1980s and early 1990s by the Canadian Hydrographic Service on behalf of the IHO and IOC.

Subsequently, contours from the Fifth Edition map sheets were digitized and included in the GEBCO Digital Atlas, which was initially released on CD-ROM in 1994 [Jones, 1994]. The Centenary Edition of the Digital Atlas [Intergovernmental Oceanographic Commission, International Hydrographic Organization, and British Oceanographic Data Centre, 2003] included the GEBCO One Minute Grid. This global grid was based on the digitized contours from the Fifth Edition, and it was the first grid released by GEBCO. The first version of

©2015. The Authors.

This is an open access article under the terms of the Creative Commons Attribution-NonCommercial-NoDerivs License, which permits use and distribution in any medium, provided the original work is properly cited, the use is non-commercial and no modifications or adaptations are made.

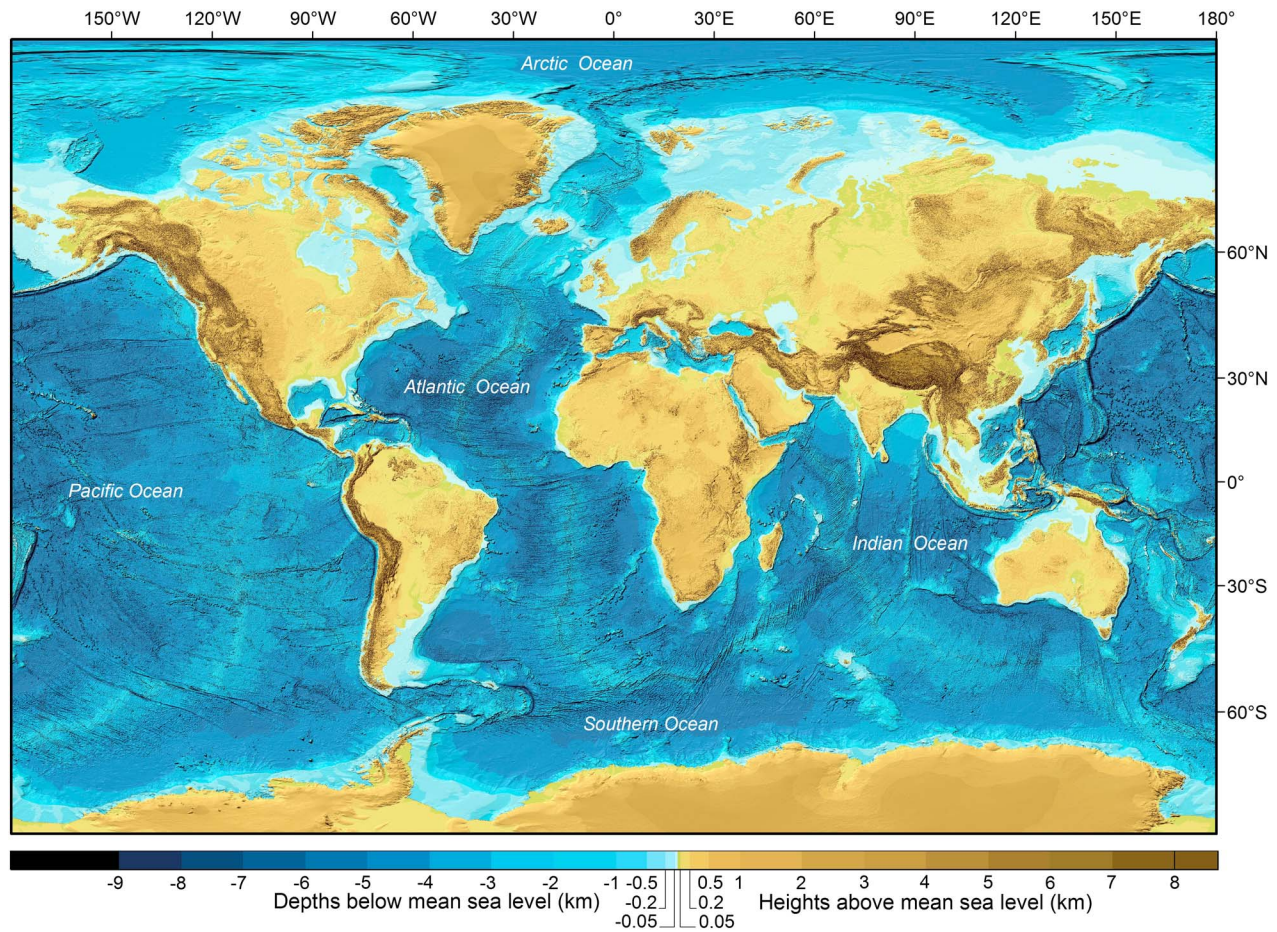


Figure 1. GEBCO_2014 grid. The colors denote ocean floor (blues) and land (browns).

the GEBCO grid to incorporate an altimetric bathymetry model (SRTM30_PLUS, [Becker *et al.*, 2009]) was released in January 2009 as “GEBCO_08.” The altimetric bathymetry model served as an underlying base grid over which regional bathymetric compilations and additional depth soundings were merged. The history of the first 100 years of GEBCO [Carpine-Lancre *et al.*, 2003] is available online (http://www.gebco.net/data_and_products/history_of_gebco/).

Here we present “GEBCO_2014,” a new version of the GEBCO global bathymetry model portraying the world ocean floor at a grid spacing of 30 arc sec (Figure 1). The grid is the result of an international collaboration of bathymetric data providers and grid developers at institutional, national, and regional levels. It includes recently released regional compilations such as the International Bathymetric Chart of the Southern Ocean (IBCSO) [Arndt *et al.*, 2013], the International Bathymetric Chart of the Arctic Ocean (IBCAO) [Jakobsson *et al.*, 2012], the Baltic Sea Bathymetry Database (BSBD) [Hell and Öiås, 2014], and the European Marine Observation and Data Network (EMODnet) 2013 database for European waters [Schaap and Moussat, 2013; Schmitt and Weatherall, 2014] (<http://www.emodnet-bathymetry.eu>).

Although GEBCO_2014 covers the globe with a 30 arc sec grid, only about 18% of the grid cells over the oceans are constrained by measured data or preprepared grids which may contain some interpolated values. In previously released GEBCO_08, it was not possible to calculate the level of constraint due to lack of source data information, i.e., metadata. GEBCO_2014 is not only improved with respect to source data density compared to previously released versions, but its companion Source Identifier (SID) grid provides metadata that includes contributor source attribution as well as constraint information. Even though the GEBCO bathymetric database has grown substantially over the last decade, the majority of the deep ocean basins as well as the Arctic and Antarctic regions remain sparsely mapped [Smith, 1993; Wessel and Chandler, 2011].

Table 1. Sources of Data Included in GEBCO_2014

Ocean Area	Regional and Global Bathymetric Grids
Gridded bathymetric data set for all ocean regions	SRTM30_PLUS, version 5.0 [Becker <i>et al.</i> , 2009]
Arctic Ocean (north of 64°N)	International Bathymetric Chart of the Arctic Ocean (IBCAO) v3 [Jakobsson <i>et al.</i> , 2012] (www.ibcao.org)
Southern Ocean (south of 60°S)	International Bathymetric Chart of the Southern Ocean (IBCSO) v1 [Arndt <i>et al.</i> , 2013] (www.ibcso.org)
Caspian Sea	Gridded data set provided by John K. Hall. [Hall, 2002]—also included in GEBCO_08
Black Sea	Gridded data set provided by John K. Hall. [Hall, 2002]—also included in GEBCO_08
Weddell Sea	Bathymetric Chart of the Weddell Sea, grid provided by the Alfred Wegener Institute for Polar and Marine Research [Schenke <i>et al.</i> , 1997]—also included in GEBCO_08
Waters around Europe	European Marine Observation and Data Network (EMODnet), 2013 data set (http://www.emodnet.eu/bathymetry)
Baltic Sea area	Baltic Sea Hydrographic Commission (2013, Baltic Sea Bathymetry Database version 0.9.3, http://data.bshc.pro)
Waters around Australia	Australian Bathymetry and Topography Grid, June 2009; supplied by Geoscience Australia [Whiteway, 2009]
Bathymetry data for all ocean regions	The Global Multi-Resolution Topography synthesis, provided by the Lamont-Doherty Earth Observatory at Columbia University (http://www.marine-geo.org/portals/gmrt/) [Ryan <i>et al.</i> , 2009]
Northwestern Pacific Ocean region	Gridded bathymetry data set provided by the Japan Oceanographic Data Center (JODC) of the Japan Coast Guard
South China Sea region	Sounding data extracted from Electronic Navigation Charts (ENCs), provided by the East Asia Hydrographic Commission
North American Great Lakes	Bathymetric grids provided by the U.S. National Oceanic and Atmospheric Administration (NOAA), National Geophysical Data Center (http://www.ngdc.noaa.gov/mgg/greatlakes/greatlakes.html)
North Atlantic Ocean, Gulf of Cadiz region	Bathymetric compilation produced under the European Science Foundation EuroMargins SWIM project “Earthquake and Tsunami hazards of active faults at the Southwest Iberian Margin: Deep structure, high-resolution imaging, and paleoseismic signature.” [Zitellini <i>et al.</i> , 2009]
Indian Ocean, region off Sumatra	Bathymetric survey carried out by HMS Scott in 2005. [Henstock <i>et al.</i> , 2006]
Waters off the west coast of Africa and waters off the Northwest European Continental Shelf area	Bathymetry data from Olex AS (http://www.olex.no/)
South Pacific Ocean, Coral Sea region	Soundings provided by Geoscience Australia (on behalf of the data set originators at the University of Sydney) for data from R/V <i>Southern Surveyor</i> (survey code SS2012_v06) and The Royal Australian Navy, Australian Hydrographic Service for data from hydrographic surveys of the region
Waters off Chile	Soundings from Electronic Navigation Charts (ENCs) supplied by the Chilean Navy Oceanographic and Hydrographic Service.
Land Area	Sources of Data for Land Areas
Regions outside of the area covered by the IBCAO and IBCSO data sets	SRTM30 from the U.S. National Aeronautics and Space Administration (NASA) Shuttle Radar Topography Mission [Farr <i>et al.</i> , 2007] (http://www2.jpl.nasa.gov/srtm/)
For the Arctic region north of 64°N	For this area land data are largely taken from the Global Multi-resolution Terrain Elevation Data 2010 (GMTED2010) data set [Danielson and Gesch, 2011]. Over Greenland the approximately 2000 × 2000 m resolution digital elevation model published by Ekholm [1996] is used.
For Antarctic regions south of 60°S	Land and ice shelf regions are based on the Bedmap2 data sets. [Fretwell <i>et al.</i> , 2013]

Much of the bathymetric data from these regions are older and poorly navigated [Smith, 1993], leaving huge areas of the world ocean floor unsounded with modern multibeam technology.

2. Methods and Data Sources

2.1. Data Sources

The GEBCO_2014 grid is a product of ongoing efforts by the GEBCO community to compile all available bathymetric data into a global gridded model. Most, but not all, of the data used in the grid are public, and their accuracy flows from that of the contributed data. These bathymetric data have been merged with land topography data to form a continuous terrain model that assumes that all data are referenced to mean sea level. However, some contributed data may have been referenced to other vertical datum; i.e., historical deep-sea multibeam surveys may have been measured relative to sea surface height, and soundings digitized from nautical charts are commonly tied to a local chart datum. Depth inconsistencies may arise from these vertical datum differences, but they are minor considering the relatively coarse GEBCO_2014 grid resolution of 30 arc sec. Table 1 lists the publicly available regional bathymetric compilations and the digital terrain model data that were used, along with their references. Bathymetry surveys over some continental shelves have been incorporated to improve shallow water portrayal.

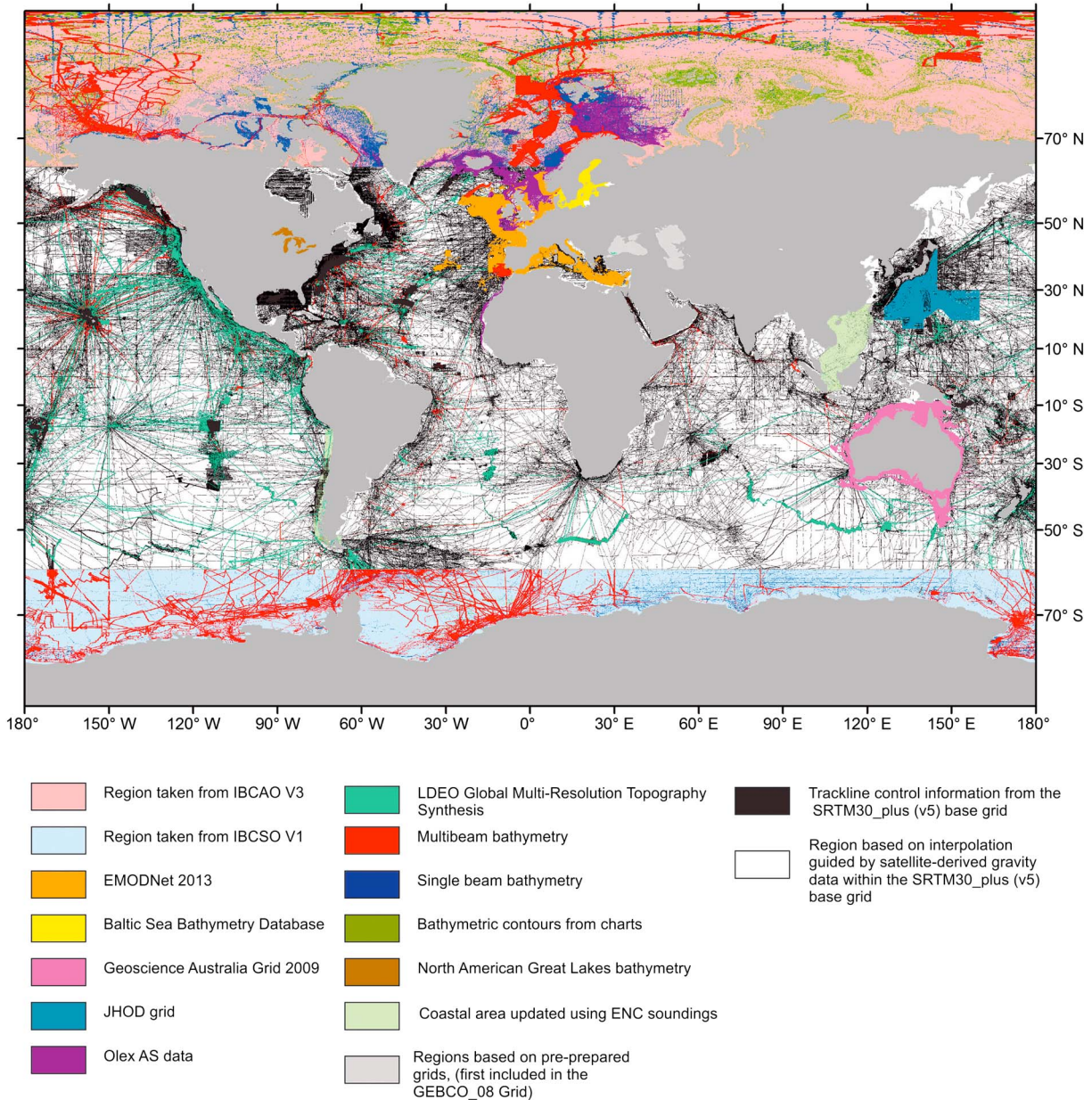


Figure 2. Regional compilations and data sets used in GEBCO_2014. The colored grid cells are constrained by soundings or existing grids. The white cells are interpolated from satellite altimetry.

Regional compilations (e.g., IBCSO, IBCAO, BSBD, and EMODnet) cover approximately 25% of the world ocean area in GEBCO_2014. In the sparsely surveyed deep ocean basins, GEBCO_2014 relies heavily on depth values derived using the satellite altimetry method. Figure 2 shows the data sources used in GEBCO_2014. We provide details on these data sources and their providers below.

2.1.1. Regional Seafloor Mapping Contributions

Recognizing the importance of local expertise when building a global bathymetric model, GEBCO set up the Sub-Committee on Regional Undersea Mapping (SCRUM) to build a close collaboration with regional mapping efforts to coordinate and encourage the inclusion of their compilations into GEBCO. The GEBCO grid has benefited from this initiative and includes compilations from IBCAO and IBCSO and waters around Europe from EMODnet and BSBD. In addition, a regional grid developed by the Japan Hydrographic Oceanographic Department has been made available through the Japan Oceanographic Data Center (JODC). This substantially improved the portrayal of the northwestern Pacific Ocean region in GEBCO_2014

compared to previously released versions. Details about SCRUM and GEBCO's regional mapping work can be found in GEBCO's website: http://www.gebco.net/regional_mapping/mapping_projects/.

The new GEBCO grid also includes data provided by some of the International Hydrographic Organization's Member States and Regional Hydrographic Commissions in the form of soundings extracted from Electronic Navigation Charts (ENCs). Gridded multibeam data compiled by the Lamont-Doherty Earth Observatory of Columbia University [Ryan *et al.*, 2009], and a form of crowd-sourced bathymetry collected by fishery vessels and compiled by Olex AS (<http://www.olex.no>), are also included.

2.1.2. Altimetric Bathymetry

Altimetry is still crucial for seafloor mapping of the remote and deep parts of the world ocean because it is capable of generating estimated depths to fill gaps between sparse ship soundings. Seafloor depths are inferred through an algorithm using gravity anomalies that in turn are derived from altimeter measurements of sea surface height. It does not provide as reliable depths as echo sounders, but the method is superior (and objective) compared to interpolation between sparse ship tracks by mathematical algorithms and hand contouring [Smith and Sandwell, 2004]. The bathymetry model that has been used as an underlying base grid in GEBCO_2014 is version 5.0 of SRTM30_PLUS [Becker *et al.*, 2009]. This model has a grid cell spacing of 30 arc sec and extends between 90°N and 90°S. It has been compiled from more than 290 million edited soundings and version 11.1 of Smith and Sandwell's [1994, 1997] bathymetry grid.

2.1.3. Bathymetric Soundings

The sources of soundings used in SRTM30_PLUS (version 5.0) are detailed in Becker *et al.* [2009]. They listed 10 of the largest compilation sources, which are (1) Marine Geophysical Trackline Data (GEODAS) archived at the IHO Data Center for Digital Bathymetry, (2) gridded swath multibeam bathymetry data cleaned and compiled as part of the Global Multi-Resolution Topography Synthesis at the Lamont-Doherty Earth Observatory of Columbia University, (3) swath multibeam data from Scripps Institution of Oceanography, (4) classified data from the National Geospatial Intelligence Agency, (5) multibeam data from the Japan Agency for Marine-Earth Science and Technology, (6) grids from the NOAA Coastal Relief Model and NOAA Coral Reef Conservation Program, (7) proprietary raw sounding data from the Institut Francais de Recherche pour L'Exploitation de la Mer, (8) "Law of the Sea" multibeam grids from the Center for Coastal and Ocean Mapping/Joint Hydrographic Center at the University of New Hampshire, (9) shallow water soundings contributed to GEBCO from hydrographic offices worldwide, and (10) data from the U.S. Naval Oceanographic Office.

Additional soundings and individual grids are regularly added to the GEBCO grid. These data are digitally incorporated using procedures such as remove-restore [Hell and Jakobsson, 2011; Smith and Sandwell, 1997] described below. These data set additions are listed in Table 1.

2.1.4. Land Topography

Except for the polar regions, land data are based on topography derived from version 2.0 of the SRTM30 gridded digital elevation model (<http://www2.jpl.nasa.gov/srtm/>), created with data from the U.S. National Aeronautics and Space Administration (NASA) Shuttle Radar Topography Mission (SRTM) [Farr *et al.*, 2007]. For the Arctic region north of 64°N, land data from IBCAO version 3.0, which is incorporated into the GEBCO grid, are from the Global Multi-resolution Terrain Elevation Data 2010 (GMTED2010) data set [Danielson and Gesch, 2011]. Over Greenland, the approximately 2 km resolution digital elevation model published by Ekholm [1996] is used. For the Southern Ocean area, south of 60°S, land data are from the ice surface topography layer of the Bedmap2 data set [Fretwell *et al.*, 2013], as included in the ice surface version of IBCSO.

2.2. Source Identification

To provide users of the global model with some indication of what the GEBCO grid is based on in a particular area, we make available a Source Identifier (SID) grid (Figure 2). This shows which of the corresponding cells in the GEBCO bathymetric grid are based on soundings, existing grids, or other data sources and which are estimated with the help of satellite altimetry or via an interpolation method. Each cell in the SID grid has an associated SID code (see User Guide to the GEBCO_2014 grid; http://www.gebco.net/data_and_products/gridded_bathymetry_data/). The code ties the corresponding topographic value in the GEBCO grid to its source—for example, over land, it is tied to the digital elevation model, over ocean, to the particular bathymetry data set or survey, such as those listed in Table 1.

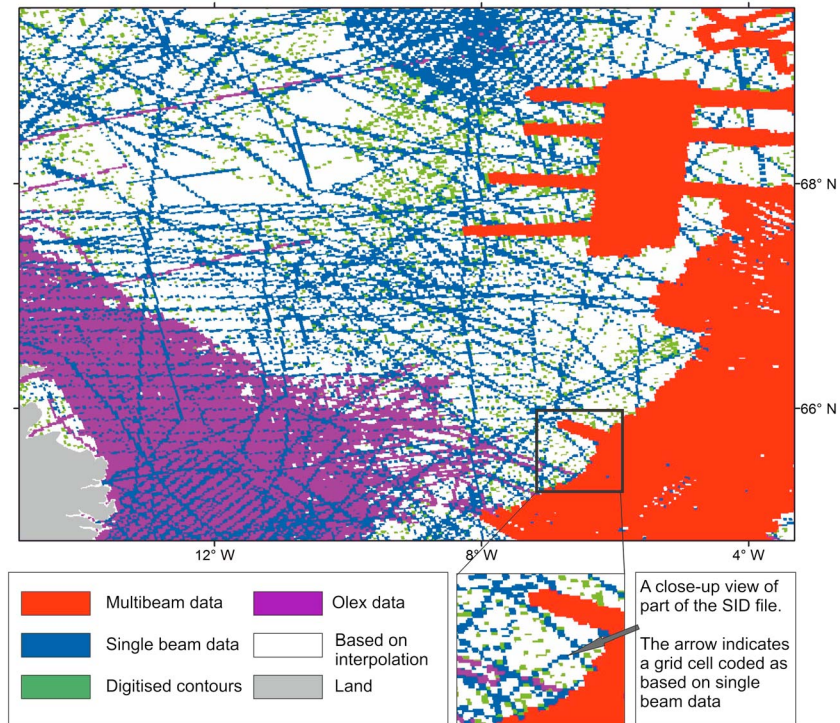


Figure 3. Image based on the Source Identifier (SID) grid (enlarged area from Figure 2). The SID grid can be used to identify the source data used to generate the GEBCO_2014 grid for individual grid cells.

Figure 3 shows an enlargement of the SID grid coverage in an area of the Norwegian Sea northeast of Iceland. IBCAO covers this area, and the SID information shown is from IBCAO. It can be seen that digitized contour lines have been incorporated along with other types of data.

2.3. Gridding and Updating

Many of the new bathymetric data sets included in this release of the GEBCO grid are from grids provided by project groups collaborating with GEBCO (Table 1). They have largely been included in the GEBCO grid using the “remove-restore” procedure [Hell and Jakobsson, 2011; Smith and Sandwell, 1997]. In Figure 4, we illustrate the remove-restore procedure in a section of the Mediterranean Sea, in which dense multibeam data from EMODnet have been incorporated into GEBCO_2014. The bottom layer is the GEBCO_08 grid, which here has only widely spaced sounding constraints. The middle layer is a grid interpolated from the difference values obtained by removing GEBCO_08 depths from EMODnet multibeam depths. The GEBCO_08 grid is then restored to the interpolated differences, forming the GEBCO_2014 grid (top layer). The remove-restore procedure both optimizes the preservation of details of the higher-resolution data while giving a smooth transition with the surrounding base grid. Indeed, fine-scale seafloor details that are only hinted at in GEBCO_08 are resolved in GEBCO_2014. This methodology has been used in the development of the IBCAO and IBCSO gridded data sets. Details of the development of the IBCAO grid (including scripts) can be found in chapter 8.2.11 of the *IHO-IOC GEBCO Cook Book* [2014]. The spline parameters used are described in the individual release articles for the regional compilations.

Data sets for updating the GEBCO grid have also been supplied in the form of individual soundings, e.g., soundings from Electronic Navigation Charts (ENCs). These data, along with additional survey data in the area, were combined and then gridded using an adjustable tension continuous curvature gridding algorithm “surface” from the Generic Mapping Tools system [Wessel and Smith, 1998; Smith and Wessel, 1990]. These grids were then added to GEBCO_2014 using the remove-restore procedure or other techniques.

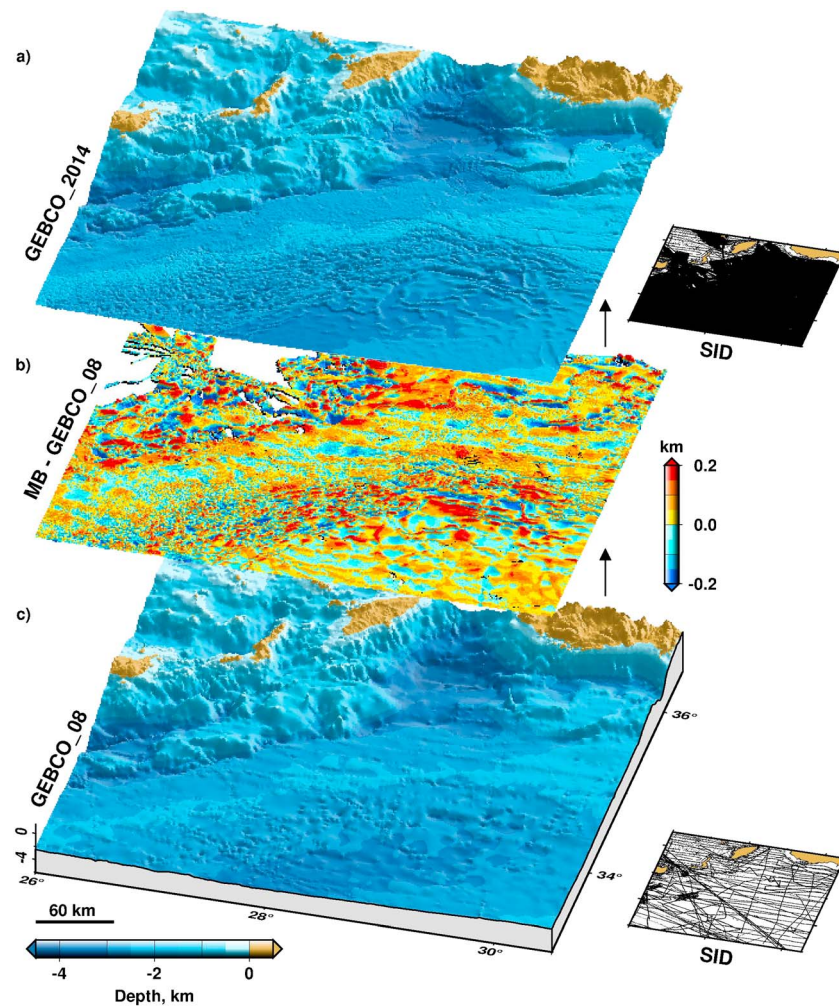


Figure 4. Example of how multibeam data are ingested into the GEBCO_2014 grid using the remove-restore procedure. The (b) differences between GEBCO_08 and multibeam data are added to (c) GEBCO_08 to form the (a) new GEBCO_2014 grid. SID maps demonstrate the improved sounding coverage.

3. Results and Discussion

GEBCO_2014 provides a more detailed portrayal of the world ocean floor than GEBCO_08. This is due not only to the updated regional compilations and additional track line data that together comprise approximately 33% of the 30 arc sec grid cells for the entire world ocean area but also to adding a large amount of individual bathymetric data. Bathymetric surveys on a finer spacing than the 30 arc sec grid have also been incorporated using the remove-restore method to enhance fine-scale details. This process will continue as new data become available, enabling incremental updates to the GEBCO grid. However, where the bathymetric grid depends on depths estimated from altimetry, the physical limitations of satellite data collection impact the resolution of gravity anomalies arising from seafloor structures.

3.1. Improvements in GEBCO_2014

Major improvements in the new GEBCO_2014 depth grid (Figure 1) can be found for

1. The two polar regions where the new IBCAO and IBCSO grids are incorporated
2. Around the European waters (Mediterranean, North, and Baltic Seas; Atlantic Ocean; and English Channel)
3. The North American Great Lakes
4. Southeast of Japan
5. Around Australia
6. Along the coasts of Chile

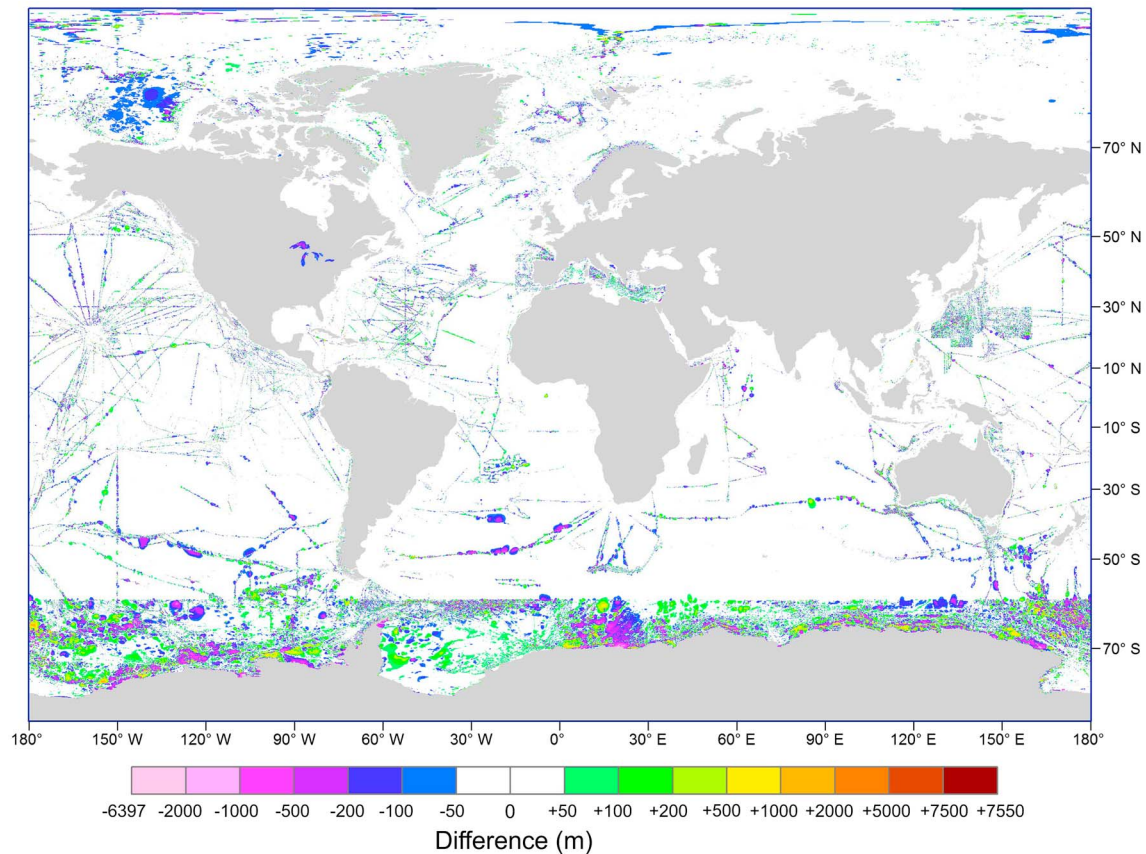


Figure 5. Depth differences obtained by subtracting GEBCO_08 from GEBCO_2014. The positive values represent deeper depths in GEBCO_08 than in GEBCO_2014.

- 7. Along the Atlantic coasts of northern Africa
- 8. Along a large number of sparse track lines crossing all the oceans.

These improvements in GEBCO_2014 as compared to GEBCO_08 are emphasized in Figure 5, which shows the differences between the two grids. The differences range from about -6400 m to $+7550$ m, and they are greatest in the areas of regional compilations such as IBCAO in the Arctic Ocean and IBCSO in the Southern Ocean. Most of the changes in IBCAO are directly related to the incorporation of new data, although some minor differences may also be due to improvements in the gridding algorithm used in IBCAO version 3.0 [Jakobsson *et al.*, 2012] (included in GEBCO_2014), over the older algorithm used in IBCAO version 2.0 [Jakobsson *et al.*, 2008] (included in GEBCO_08).

The large and widespread differences in the Southern Ocean revealed by the difference grid are due to IBCSO version 1.0 being the first regional compilation released covering this entire area. While GEBCO_08 relied much more on satellite altimetry in the Southern Ocean, the significantly increased number of sounding data improved the newly modeled bathymetry in IBCSO version 1.0. In addition, IBCSO did not use satellite altimetry for its southernmost areas due to methodology limitations of satellite altimetry in polar regions. In the remaining areas IBCSO used a newly developed gridding algorithm that adjusts the satellite altimetry to the sounding data. Further, at the ocean-continent transition of the Antarctic coastline, significant improvements have been achieved with the usage of bedrock topography in the creation of the original IBCSO grid instead of ice surface topography.

Another way of expressing changes between GEBCO_2014 and GEBCO_8 is illustrated in Figure 6, where the following relation is expressed:

$$\frac{Abs(GEBCO_08 - GEBCO_2014)}{GEBCO_2014} \times 100 \tag{1}$$

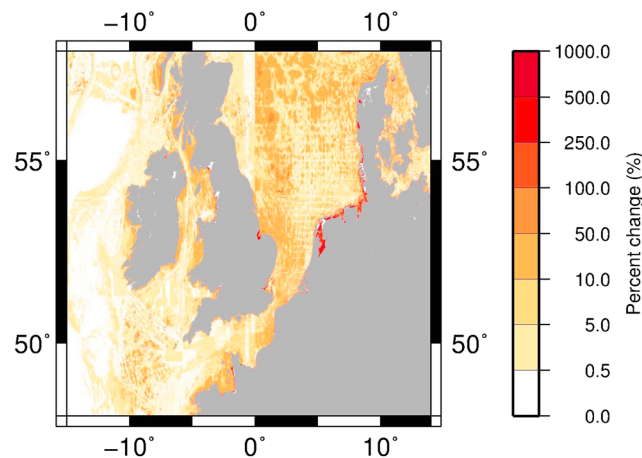


Figure 6. Percentage of changes between GEBCO_2014 and GEBCO_08 grids in North Sea region.

This measure can be understood as the percentage of vertical changes reported in GEBCO 2014, which is considered to be the reference. Changes smaller than 0.5% are practically imperceptible at the scale of the GEBCO compilation. The greatest changes generally occur along the coasts, particularly in bays (e.g., note the bays along the German coast in Figure 6). The calculated change values may look excessive in some areas, exceeding 1000%. However, these change values are interpreted to be related to both the limitation of the altimetry-driven interpolation along the coasts and the incorporation of new soundings or data from existing

bathymetric grids in these areas where no soundings at all were available during the compilation of GEBCO_08. Moreover, expressing changes between the two grids with the equation above emphasizes the need of highly accurate bathymetric data in coastal and shallow areas.

3.2. Limits of Satellite Altimetry

The resolution that may be achieved by satellite altimetry depends primarily on the regional ocean depth. This is due to Newton's law and is known as upward continuation. As a rule of thumb, the smallest seafloor feature that can be resolved is about $\pi \times$ water depth, so for oceans that average 4 km in depth, features smaller than about 12 km wide are not easily resolved. However, slightly smaller (11 km wide) features may be resolved at shallower (~2.5–3 km) ocean depths [Marks *et al.*, 2013], and the latest gravity fields that incorporate new altimeter data are improving accuracy particularly in the 12 to 40 km wavelength band [Sandwell *et al.*, 2014]. Previous studies found that seamounts less than about 2 km tall are poorly resolved in gridded marine gravity fields [e.g., Kim and Wessel, 2011; Wessel, 2001; Wessel and Lyons, 1997]. But along-track coherence between AltiKa and multibeam data shows that over the East Pacific Rise, 1 km tall seamounts that are 10 km in width can be resolved [Smith, 2015], but due to gridding and cross-track spacing, signals from seamounts this small are not consistently resolved in marine gravity fields.

Another limiting factor is the satellite track density. Although data collected along an altimeter track may be dense, the distance between tracks limits the resolution—the wider the spacing the poorer the resolution. Adding data from satellites with different inclinations helps fill the spaces between tracks and enhances the east-west component of resolution. There are also limitations due to altimeter technology [Sandwell *et al.*, 2014].

In the high latitudes of the Arctic and Southern Ocean, special limitations apply. The satellite inclination limits the spatial coverage of satellite altimetry data, and the presence of year-round sea ice reduces the signal quality [Schöne and Schenke, 1998]. Hence, the usage of satellite altimetry data in the polar regional compilations of IBCAO and IBCSO is restricted in coverage.

3.3. Bathymetry Model Resolution

The resolution of the bathymetry model is a function of the underlying data density—the coverage of satellite tracks for depth estimates and ship soundings. Multibeam surveys collect depth measurements at very high density and may be designed with overlapping swaths to provide full map coverage. When multibeam data are incorporated into the bathymetry model, their high data density improves the resolution of seafloor details.

We illustrate this in Figure 7a, which shows the GEBCO_2014 model over a portion of the southern Mid-Atlantic Ridge. Figure 7b shows the locations of bathymetric soundings used in the model. We compare

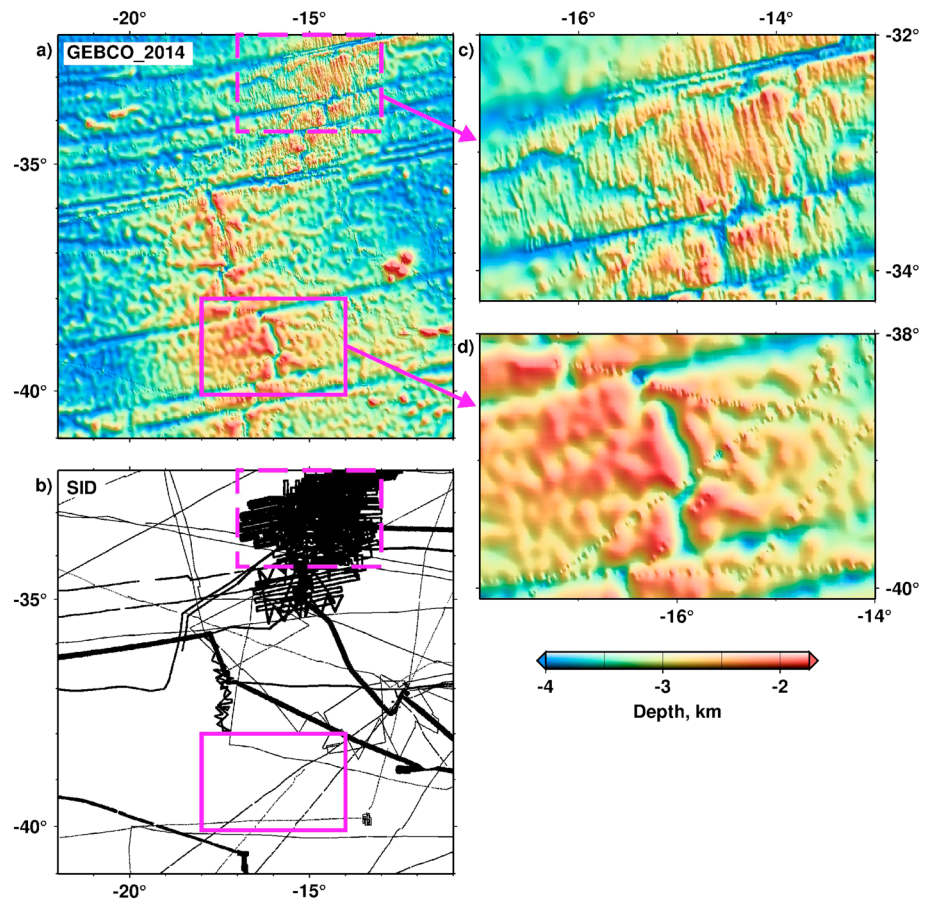


Figure 7. (a) GEBCO_2014 bathymetry model over the southern Mid-Atlantic Ridge and (b) locations of depth constraints used in model. North-south trending abyssal hills flanking the spreading ridge axis are resolved in Figure 7a (dashed box) and enlargement (c) because multibeam data were incorporated into the bathymetry model. (d) Abyssal hill fabric is only hinted at where depths are estimated primarily from satellite altimetry.

two areas on the ridge—one that has been surveyed by multibeam [Michael *et al.*, 1994] (dashed box) and the other with soundings from only a few ship tracks (solid box). Abyssal hills, which run parallel to ridge axes, are narrow, low-relief horsts and grabens (2–5 km wide, 50–300 m high) [Macdonald *et al.*, 1996] that are abundant on the flanks of the Mid-Atlantic spreading ridge [Goff *et al.*, 1995]. The abyssal hill details are evident in the incorporated multibeam survey (Figure 7c). A nearby segment of the spreading ridge (solid box in Figure 7a and enlarged in Figure 7d), that has depths estimated primarily from altimetry, shows only a hint of abyssal hill fabric. The abyssal hills in Figure 7d are not resolved in the same detail because depths estimated from altimetry cannot resolve such small features due to the altimeter track spacing, the water depth, and the paucity of soundings (solid box in Figure 7b). However, large features such as spreading ridge segments and fracture zones that offset them are mapped by the bathymetry model even where there are large gaps between soundings, because depths estimated from altimetry have filled the gaps.

3.4. Hypsometry of the World Ocean

Hypsometry refers to the area distribution of depth or height. A hypsometric curve is thus a histogram of heights or depths over a certain region [Langbein, 1947]. Such a curve is commonly used as a base for description of a region’s morphology and geological evolution. With the very limited information available at the beginning of the twentieth century, the world ocean hypsometry was calculated by Murray and Hjort [1912]. The maps underlying their study were compiled by Murray from all available soundings that, at the time, amounted to 5962. The hypsometry was calculated over intervals of 1000 fathoms, and they concluded that largest portion, making up 47.29% of the total world ocean area, consisted of depths

between 1000 and 2000 fathoms (1828 and 3657 m). In the classic work by *Menard and Smith* [1966], the world ocean hypsometry was analyzed using the most recent Russian and U.S. bathymetric maps available at the time of the study. They concluded that their derived hypsometric curve differed little from that published by *Murray and Hjort* [1912]. This is somewhat surprising considering that 54 years passed between these studies and that major discoveries on the ocean floor morphology had been published [e.g., *Heezen*, 1960; *Heezen and Ewing*, 1961] during this time interval. *Smith and Sandwell* [1997] derived the hypsometry from their global seafloor topography model compiled using satellite altimetry and ship soundings. They used the hypsometric function in an innovative approach to address the age-depth-area relationship of the world ocean floor.

Anticipating that the significant increase in constrained depths in GEBCO_2014 may yield new insights, we performed a new hypsometric analysis using GEBCO_2014 and calculated some basic statistics including mean and median depth. Our analysis identifies physical characteristics that can be interpreted in light of the historical perspective of knowledge of the world ocean floor. We performed the hypsometric calculations using spherical coordinates, and for the sake of simplicity, we assume a round Earth with a radius of 6371 km.

In order to account for a sloping topography and “inclined pixels” that in fact would be larger in order to represent the area of a slope properly, we calculated the maximum inclination of each pixel in the GEBCO_2014 grid based on the surrounding depths and inferred the following area (A) correction:

$$dA_{\text{corr}} = dA / \cos(\alpha) \quad (2)$$

The general shape of the hypsometric curve representing GEBCO_2014 in Figure 8a is not much different than the curve based on the altimetric bathymetry model compiled by *Smith and Sandwell* [1997], although the calculated world ocean average and median depths differ from previous estimates. There is a trend suggesting that more recent compilations generally are shallower, which is shown by comparing the world ocean average: 3729 m [*Menard and Smith*, 1966], 3682 m [*Charette and Smith*, 2010], and 3441 m (GEBCO_2014). This may be due to a systematic bias toward finding new bathymetric highs (e.g., seamounts and ridges) in newly gathered depth surveys and in global altimetric bathymetry [*Smith and Sandwell*, 1997], in contrast to sparse sounding data that span abyssal plains where a uniform deep depth may be assumed. This was particularly true at the time when a bathymetrist manually drew depth contours based on sparse soundings. The hypsometric curve in Figure 8a shows that 50% of Earth’s surface is deeper than 3200 m. More frequently cited however is that 71% of the Earth’s surface is composed of ocean.

It is interesting to note the shape of the curve showing the area difference between slope-corrected hypsometric calculation using equation (2) and when no slope correction is applied. The percentage difference between the two is barely distinguishable, except for in the very rough topographic terrain of our highest mountain chains (Figure 8b). On a global scale, the largest absolute difference is found at an elevation of ~800 m and a depth of ~3600 m, i.e., slightly deeper than the mean depth of the world ocean.

Finally, the hypsometric analysis may be used to estimate the effort needed to survey “uncharted” areas of the world ocean using modern multibeam echosounders [*Carron et al.*, 2001]. Table 2 provides a first-order approximation effort needed. In order to estimate this value, some hypotheses needed to be considered:

1. Water depth intervals have been selected in order to roughly correspond to the technical characteristics of the different modern multibeam surveys.
2. The number of grid nodes originating from altimetry has been selected using the corresponding SID value. The number of grid nodes per water depth intervals is converted to a surface using both equation (2) and the assumption that the distribution of uncharted nodes is homogeneous latitude-wise.
3. The charting effort takes into consideration that (1) for each water depth interval, the average represents the distribution; (2) this average water depth is multiplied by a factor representing the projection of the swath width of a multibeam system on the seafloor—a conservative approach is to estimate that modern multibeam echosounders survey 3.5 times the water depth; and (3) the speed of the survey boat is considered to be 7.5 knots (~10 km/h). However, this does not take into account maneuvering, meteorological and oceanic adverse conditions, or deployment of auxiliary sensors (tide gauges principally in shallow waters and sound velocity profiling).

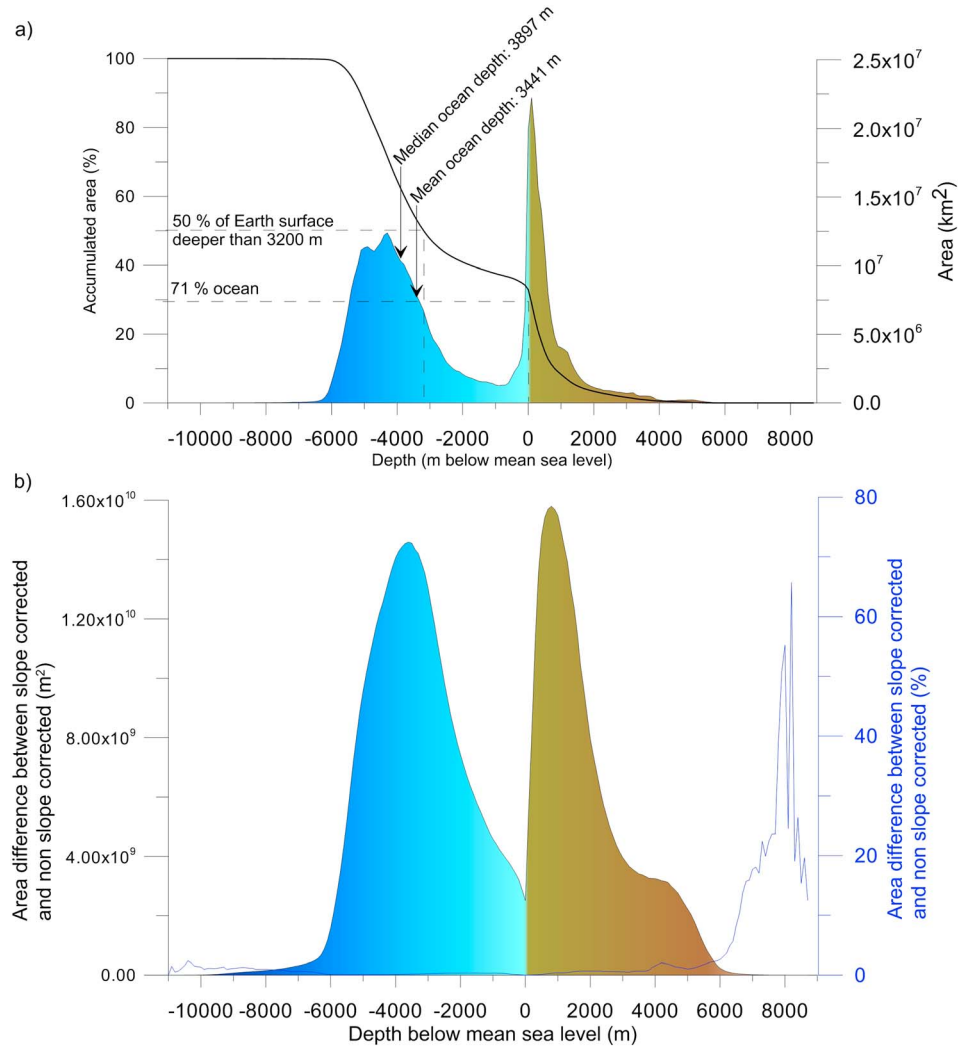


Figure 8. Earth’s hypsometry from GEBCO_2014. (a) The filled curves are the distribution of ocean depths (blue) and land elevations (brown) relative to calculated area (right y axis); the solid black line is the accumulated area in percent (left y axis). (b) Comparison between slope-corrected and nonslope-corrected hypsometric calculations, the colors are the same as in Figure 8a.

Based on our assumptions used to approximate these numbers, the results give a total effort of about 900 years of surveying for one single system, separated into about 300 years for middle and deep waters, and about 600 years for shallow waters. These values remain in the same order of magnitude as those presented by Carron *et al.* [2001] when estimating the effort of the Global Ocean Mapping Project. Selection of different working hypotheses (swath width and surveying speed) might explain some marginal differences between the values. Note must be taken that these values only take into account the

Water Depth Interval (Modal Water Depth)	Average Water Depth (km)	Proportion of Water Depth (%)	Proportion of Uncharted Surface (%)	Cumulated Surface of the GEBCO 2014 Grid Nodes Originating From Interpolated Driven by Altimetry (km ²)	Remaining Effort (Years)
>3000	4	75.3	85	230,910,385	188
3000–1000	1.5	13.0	72	34,143,193	74
1000–200	0.4	4.4	66	10,654,693	86
0–200	0.1	7.3	71	18,995,603	619

acquisition effort. While progress is being made to improve processing time [Calder and Mayer, 2001], it can still represent a fair amount of time in the life cycle of bathymetric data.

In 2003, the International Hydrographic Office compiled a list of approximately 700 systems held either by national hydrographic offices, research institutes, or private bodies in the world (IHO Circular Letter 37/2003, 27 May 2003, World list of multibeam systems, http://www.iho.int/mtg_docs/circular_letters/english/2003/CI37e.pdf). Both our evaluation of the effort and the number of systems roughly suggests that if each of the sounders would be used intensively as part of a strategic program, most of the acquisition work could be done in just over a year. Practically, Carron *et al.* [2001] indicated a time frame of 20–30 years to survey 90% of the surface of the ocean (water depths deeper than 500 m) starting from the beginning of the century. So far, in 2015, it appears that nowhere close to a half or even a third of this surface has been covered and brought to the knowledge of the GEBCO community.

The shallow waters offer the greatest practical benefits to mankind; however, they also present the greatest practical difficulties as they concentrate most of the adverse conditions (strong currents and tidal effects; danger of running aground; and high variability of the physical parameters needed to measure accurately the depth such as sound velocity, multiple concomitant usages, and political issues). Finally, the results given in Table 2 reflect only an “initial” complete coverage, but geological and oceanographic dynamic processes, especially in shallow waters, continuously modify the morphology of the seabed, which implies resurveying some areas.

4. Summary and Outlook

GEBCO_2014 is the latest version of the global digital bathymetric model that is available for free download from the Internet in commonly used formats. This updated version includes the most recent regional bathymetric compilations plus new bathymetric surveys and soundings gathered along transit ship tracks. GEBCO digital bathymetric models have been widely used over the past decade, providing users with current bathymetric information for scientific and educational use.

The ongoing success of GEBCO community effort depends on continued collaboration and cooperation with IHO Member States; regional hydrographic commissions; regional mapping groups; and research, educational, and commercial institutions. Future versions of the GEBCO bathymetry model will be improved as more bathymetric data are collected, as existing data are made publicly available, and as regional compilations are updated. New gravity fields are being constructed with new altimeter measurements that are more accurate and resolve smaller features than previous versions [Sandwell *et al.*, 2014]. This will benefit GEBCO specifically in the sparsely surveyed most remote parts of the deep world ocean. Shallow areas are also benefiting from additional data collected through “crowd sourcing”—the voluntary efforts by a number of people who have agreed to collect bathymetric data while yachting or performing other ocean-borne ship activities (e.g., Olex bathymetry).

Also as part of its activities, GEBCO seeks to provide educational materials and courses (e.g., the *IHO-IOC GEBCO Cook Book* [2014] and the Nippon Foundation/GEBCO Training Program) to help researchers of all experience levels succeed in the collection, processing, and gridding of bathymetric data. These data can be incorporated into the GEBCO grid to improve it. Through international collaboration, we can continue to help build the best publicly available global bathymetric models.

Acknowledgments

The GEBCO_2014 grid and associated products may be downloaded from <http://www.gebco.net>, and the GEBCO Digital Atlas Manager, Pauline Weatherall, may be reached at paw@bodc.ac.uk. Building the GEBCO grid is a collaborative and worldwide effort. All the bathymetrists who have contributed to describe the ocean floor are associated with this publication. The comments of J.J. Becker and an anonymous reviewer improved this manuscript. We thank Walter H.F. Smith for the helpful discussions. The views, opinions, and findings contained in the report are those of the authors and should not be construed as an official National Oceanic and Atmospheric Administration or U.S. Government position, policy, or decision.

References

- Arndt, J. E., *et al.* (2013), The International Bathymetric Chart of the Southern Ocean (IBCSO) version 1.0—A new bathymetric compilation covering circum-Antarctic waters, *Geophys. Res. Lett.*, *40*, 3111–3117, doi:10.1002/grl.50413.
- Becker, J. J., *et al.* (2009), Global bathymetry and elevation data at 30 arc seconds resolution: SRTM30_PLUS, *Mar. Geod.*, *32*(4), 355–371, doi:10.1080/01490410903297766.
- Calder, B. R., and L. A. Mayer (2001), Automatic processing of high-rate, high-density multibeam echosounder data, *Geochem. Geophys. Geosyst.*, *4*(6), 1048, doi:10.1029/2002GC000486.
- Carpine-Lancré, J., R. Fisher, B. Harper, P. Hunter, M. Jones, A. Kerr, A. Laughton, S. Ritchie, D. Scott, and M. Whitmarsh (2003), *The History of GEBCO 1903-2003, the 100-year Story of the General Bathymetric Chart of the Oceans*, GITC bv, Lemmer, Netherlands.
- Carron, M. J., P. R. Vogt, and W.-Y. Jung (2001), A proposed international long-term project to systematically map the world's ocean floors from beach to trench: GOMaP (Global Ocean Mapping Program), *Int. Hydrogr. Rev.*, *2*(3), 49–55.
- Charette, M. A., and W. H. F. Smith (2010), The volume of Earth's ocean, *Oceanography* *23*(2), 112–114, doi:10.5670/oceanog.2010.51.
- Danielson, J. J., and D. B. Gesch (2011), *Global Multi-resolution Terrain Elevation Data 2010 (GMTED2010)*, U.S. Geol. Surv., Reston, Va.

- Ekholf, S. (1996), A full coverage, high-resolution, topographic model of Greenland computed from a variety of digital elevation data, *J. Geophys. Res.*, *101*(B10), 21,961–21,972, doi:10.1029/96JB01912.
- Farr, T. G., et al. (2007), The Shuttle Radar Topography Mission, *Rev. Geophys.*, *45*, RG2004, doi:10.1029/2005RG000183.
- Fretwell, P., et al. (2013), Bedmap2: Improved ice bed, surface and thickness datasets for Antarctica, *Cryosphere*, *7*, 375–393, doi:10.5194/tc-7-375-2013.
- General Bathymetric Chart of the Oceans (GEBCO) (2010), GEBCO_08 grid, version 20100927. [Available at <http://www.gebco.net>], Br. Oceanogr. Data Cent., Liverpool, U. K.
- Goff, J. A., B. E. Tucholke, J. Lin, G. E. Jaroslow, and M. C. Kleinrock (1995), Quantitative analysis of abyssal hills in the Atlantic Ocean: A correlation between inferred crustal thickness and extensional faulting, *J. Geophys. Res.*, *100*(B11), 22,509–22,522, doi:10.1029/95JB02510.
- Hall, J. K. (2002), Bathymetric compilations of the seas around Israel I: The Caspian and Black Seas, in *Current Research*, vol. 13, edited by R. Bogosh, pp. 105–108, Geol. Surv. of Israel, Jerusalem, Israel.
- Hall, J. K. (2006), GEBCO Centennial Special Issue—Charting the secret world of the ocean floor: The GEBCO Project 1903–2003, *Mar. Geophys. Res.*, *27*(1), 1–5, doi:10.1007/s11001-006-8181-4.
- Heezen, B. C. (1960), The rift in the ocean floor, *Sci. Am.*, *203*(4), 98–110, doi:10.1038/scientificamerican1060-98.
- Heezen, B. C., and M. Ewing (1961), The mid-oceanic ridge and its extension through the Arctic Basin, in *Geology of the Arctic*, edited by G. O. Raasch, pp. 622–642, Univ. of Toronto Press, Canada.
- Hell, B., and H. Öiås (2014), A new bathymetry model for the Baltic Sea, *Int. Hydrogr. Rev.*, *P-1*, 21–32.
- Hell, B., and M. Jakobsson (2011), Gridding heterogeneous bathymetric data sets with stacked continuous curvature splines in tension, *Mar. Geophys. Res.*, *32*(4), 493–501, doi:10.1007/s11001-011-9141-1.
- Henstock, T. J., L. C. McNeill, and D. R. Tappin (2006), Seafloor morphology of the Sumatran subduction zone: Surface rupture during megathrust earthquakes?, *Geology*, *34*(6), 485–488, doi:10.1130/22426.1.
- IHO-IOC GEBCO Cook Book (2014), *The IHO-IOC GEBCO Cook Book*, p. 331, IHO Publ., B-11, Monaco–IOC Manuals and Guides 63, France.
- IOC, IHO, and BODC (2003), *Centenary Edition of the GEBCO Digital Atlas, Published on CD-ROM on Behalf of the Intergovernmental Oceanographic Commission and the International Hydrographic Organization as Part of the General Bathymetric Chart of the Oceans*, British Oceanographic Data Centre, Liverpool, U. K.
- Jakobsson, M., R. Macnab, L. Mayer, R. Anderson, M. Edwards, J. Hatzky, H. W. Schenke, and P. Johnson (2008), An improved bathymetric portrayal of the Arctic Ocean: Implications for ocean modeling and geological, geophysical and oceanographic analyses, *Geophys. Res. Lett.*, *35*, L07062, doi:10.1029/2008GL033520.
- Jakobsson, M., et al. (2012), The International Bathymetric Chart of the Arctic Ocean (IBCAO) version 3.0, *Geophys. Res. Lett.*, *39*, L12609, doi:10.1029/2012GL052219.
- Jones, M. T. (1994), *The GEBCO Digital Atlas*, pp. 17–20, NERC News, Swindon, U. K.
- Kim, S.-S., and P. Wessel (2011), New global seamount census from altimetry-derived gravity data, *Geophys. J. Int.*, *186*(2), 615–631, doi:10.1111/j.1365-246X.2011.05076.x.
- Langbein, W. B. (1947), *Topographic Characteristics of Drainage Basins*, U.S. Geol. Surv. Water Supply Pap., 968-C, U.S. Govt. Print. Off., Washington, D. C.
- Macdonald, K. C., P. J. Fox, R. T. Alexander, R. Pockalny, and P. Gente (1996), Volcanic growth faults and the origin of Pacific abyssal hills, *Nature*, *380*, 125–129, doi:10.1038/380125a0.
- Marks, K. M., W. H. F. Smith, and D. T. Sandwell (2013), Significant improvements in marine gravity from ongoing satellite missions, *Mar. Geophys. Res.*, *34*(2), 137–146, doi:10.1007/s11001-013-9190-8.
- Menard, H. W., and S. M. Smith (1966), Hypsometry of ocean basin provinces, *J. Geophys. Res.*, *71*(18), 4305–4325, doi:10.1029/JZ071i018p04305.
- Michael, P. J., et al. (1994), Mantle control of a dynamically evolving spreading center: Mid-Atlantic Ridge 31–34°S, *Earth Planet. Sci. Lett.*, *121*(3–4), 451–468, doi:10.1016/0012-821x(94)90083-3.
- Murray, J., and J. Hjort (1912), *The Depths of the Ocean: A General Account of the Modern Science of Oceanography Based Largely on the Scientific Researches of the Norwegian Steamer Michael Sars in the North Atlantic*, Macmillan and Company, London, U. K., doi:10.5962/bhl.title.6874.
- Ryan, W. B. F., et al. (2009), Global multi-resolution topography synthesis, *Geochem. Geophys. Geosyst.*, *10*, Q03014, doi:10.1029/2008GC002332.
- Sandwell, D. T., R. D. Muller, W. H. F. Smith, E. Garcia, and R. Francis (2014), New global marine gravity model from CryoSat-2 and Jason-1 reveals buried tectonic structure, *Science*, *346*(6205), 65–67, doi:10.1126/science.1258213.
- Schaap, D. M. A., and E. Moussat (2013), EMODNet Hydrography-Seabed Mapping—Developing a higher resolution digital bathymetry for the European seas, *Geophys. Res.*, Abstracts, vol. 15, EGU2013-3620, EGU General Assembly 2013, Vienna, Austria.
- Schenke, H. W., H. Hinze, S. J. Dijkstra, B. Hoppmann, F. Niederjasper, and T. Schöne (1997), A new bathymetric chart of the Weddell Sea: AWI BCWS, in *Ocean, Ice, and Atmosphere: Interactions at the Antarctic Continental Margin Antarctic Res. Ser.*, edited by S. Jacobs and R. Weiss, 75 pp., AGU, Washington, D. C., doi:10.1594/PANGAEA.708081.
- Schmitt, T., and P. Weatherall (2014), GEBCO and EMODNet—Bathymetry hand in hand: Improving global and regional bathymetric models of European waters, Abstract OS31B-0989 presented at 2014 Fall Meeting, AGU, San Francisco, Calif., 15–19 Dec.
- Schöne, T., and H. W. Schenke (1998), Gravity determination in ice covered regions by altimetry, in *Geodesy on the Move*, vol. 119, edited by R. Forsberg, M. Feissel, and R. Dietrich, pp. 156–162, Springer, Berlin, doi:10.1007/978-3-642-72245-5_21.
- Smith, W. H. F. (1993), On the accuracy of digital bathymetric data, *J. Geophys. Res.*, *98*(B6), 9591–9603, doi:10.1029/93JB00716.
- Smith, W. H. F. (2015), The resolution of seamount geoid anomalies achieved by the SARAL AltiKa and Envisat RA2 satellite radar altimeters, *Mar. Geod.*, doi:10.1080/01490419.2015.1014950.
- Smith, W. H. F., and D. T. Sandwell (1994), Bathymetric prediction from dense satellite altimetry and sparse shipboard bathymetry, *J. Geophys. Res.*, *99*(B11), 21,803–21,824, doi:10.1029/94JB00988.
- Smith, W. H. F., and D. T. Sandwell (1997), Global sea floor topography from satellite altimetry and ship depth soundings, *Science*, *277*(5334), 1956–1962, doi:10.1126/science.277.5334.1956.
- Smith, W. H. F., and D. T. Sandwell (2004), Conventional bathymetry, bathymetry from space, and geodetic altimetry, *Oceanography*, *17*(1), 8–23, doi:10.5670/oceanog.2004.63.
- Smith, W. H. F., and P. Wessel (1990), Gridding with continuous curvature splines in tension, *Geophysics*, *55*(3), 293–305, doi:10.1190/1.1442837.
- Wessel, P. (2001), Global distribution of seamounts inferred from gridded Geosat/ERS-1 altimetry, *J. Geophys. Res.*, *106*(B9), 19,431–19,441, doi:10.1029/2000JB000083.

- Wessel, P., and M. T. Chandler (2011), The spatial and temporal distribution of marine geophysical surveys, *Acta Geophys.*, 59(1), 55–71, doi:10.2478/s11600-010-0038-1.
- Wessel, P., and S. Lyons (1997), Distribution of large Pacific seamounts from Geosat/ERS-1: Implications for the history of intraplate volcanism, *J. Geophys. Res.*, 102(B10), 22,459–22,475, doi:10.1029/97JB01588.
- Wessel, P., and W. H. F. Smith (1998), New, improved version of generic mapping tools released, *Eos Trans. AGU*, 79(47), 579, doi:10.1029/98EO00426.
- Whiteway, T. (2009), *Australian Bathymetry and Topography Grid*, June 2009, Scale 1:5000000, Geoscience, Australia, Canberra, doi:10.4225/25/53D99B6581B9A.
- Zitellini, N., et al. (2009), The quest for the Africa-Eurasia plate boundary west of the Strait of Gibraltar, *Earth Planet. Sci. Lett.*, 280(1–4), 13–50, doi:10.1016/j.epsl.2008.12.005.